Eur Arch Psychiatry Clin Neurosci (2004) 254 : 190–198 DOI 10.1007/s00406-004-0469-2

ORIGINAL PAPER

C. Mulert · O. Pogarell · G. Juckel · D. Rujescu · I. Giegling · D. Rupp · P. Mavrogiorgou · P. Bussfeld · J. Gallinat · H. J. Möller · U. Hegerl

The neural basis of the P300 potential

Focus on the time-course of the underlying cortical generators

Received: 5 February 2003 / Accepted: 6 October 2003

Abstract The locations and time-courses of the neural generators of the event-related P300 potential have been well described using intracranial recordings. However, this invasive method is not adequate for usage in healthy volunteers or psychiatric patients and not all brain regions can be covered well with this approach. With functional MRI, a non-invasive method with high spatial resolution, most of these locations could be found again. However, the time-course of these activations can only be roughly determined with this method, even if an event-related fMRI design has been chosen. Therefore, we have now tried to analyse the time-course of the activations using EEG data providing a better time resolution. We have used Low Resolution Electromagnetic Tomography (LORETA) in the analysis of P300 data (27 electrodes) of healthy volunteers (n = 50) in the time frame 230–480 ms and found mainly the same activations that have been described using intracranial recordings or fMRI, i. e. the inferior patrietal lobe/temporo-parietal junction (TPJ), the supplementary motor cortex (SMA) and the anterior cingulate cortex (ACC), the superior temporal gyrus (STG), the insula and the dorsolateral prefrontal cortex. In these selected regions, an analysis of the activation time-courses has been performed.

Key words P300 · evoked potential · LORETA

C. Mulert (✉) · O. Pogarell · G. Juckel · D. Rujescu · I. Giegling · D. Rupp · P. Mavrogiorgou · P. Bussfeld · J. Gallinat · H. J. Möller · U. Hegerl
Laboratory for Clinical Neurophysiology
Dept. of Psychiatry
Nußbaumstraße 7
80336 München, Germany
Tel.: +49-89/5160-3392
Fax: +49-89/5160-5542
E-Mail: cmulert@psy.med.uni-muenchen.de

EAPCN 469

Introduction

The event-related P300 potential has been widely used in neurophysiological research (Dierks and Maurer 1989; Hegerl et al. 1995; Frodl-Bauch et al. 1999; Winterer et al. 2001). It is usually evoked with an oddball paradigm. Stimuli (for example, tones) are presented in a way that one stimulus is rare and relevant (for example, a button must be pressed), and another stimulus is often presented, but irrelevant. The P300 potential is then recorded widely across the scalp some 300 ms after the rare stimulus. One main reason for the broad application in neurophysiological research is the fact that, in several brain/mental diseases like Alzheimer disease or schizophrenia, attenuations of the P300 amplitude and latency have been described (Roth and Cannon 1972; Juckel et al. 1996; Higashima et al. 1998; Blackwood 2000; Gallinat et al. 2001). Since the earlier part of the P300, the more novelty-sensitive P3a is more frontally pronounced and the later (main) part of the P300, the P3b, has a parietal maximum, a rough assignment of the described patterns to the generating brain structures has been possible. However, a precise correlation of the scalp data to the underlying brain regions was not possible, since the correct localisation of the generators of scalp-measured EEG data was limited due to the low spatial resolution of EEG data. Attempts in this direction with traditional source analyses have permitted only rough estimates of the generating brain structures (Hegerl and Frodl-Bauch 1997). Good evidence with regard to the electrical generators has been provided by intracranial investigations (Halgren et al. 1998). However, this invasive method is not adequate for usage in healthy volunteers or psychiatric patients, not all brain regions can be covered well with this approach and the contribution of potentials recorded intracranially to the scalp potentials is not clear. Finally, the upcoming of functional imaging technologies has been an important methodological advantage. With the availability of modern, non-invasive imaging technologies like functional

Magnetic Resonance Imaging (fMRI), the underlying brain activations in an oddball task could largely be detected (McCarthy et al. 1997; Menon et al. 1997; Linden et al. 1999; Clark et al. 2000; Downar et al. 2000; Stevens et al. 2000; Kiehl et al. 2001; Horn et al. 2003), i. e., it could be confirmed that main activations are in the temporo-parietal junction, the STG, the SMA and ACC, the insula and the dorsolateral prefrontal cortex (Table 1). Therefore, the question of the locations of the generators has been largely resolved and a high degree of accordance could be seen between intracranial recordings and fMRI investigations (there remain some open questions, like the contribution of medial temporal lobe structures/hippocampus). This allows the usage of the non-invasive fMRI in clinical and research applications with regard to the localisation of P300 generators. The next point of interest is the time-course of activation, i. e. the sequence and dynamics of brain activity. However, although the spatial resolution of fMRI is excellent, the time resolution is restricted. This is particularly true for block design studies. With an event-related design, some statements about the time-course of brain activation have become possible (Burock et al. 1998; Friston et al. 1998), but also event-related studies have a time resolution far from the time resolution of EEG and evoked potentials. Therefore, for an improved understanding of the dynamical brain activity underlying the P300 potential, investigations are missing that offer high time resolution and acceptable spatial resolution. Here again, EEG comes into play. However, the first and crucial point for an EEG-based analysis would be to describe the locations of the electrical generators correctly, that is, in high accordance with the results known from fMRI experiments. However, if this precondition is fulfilled, a step beyond localisation could be made in analysing the time-course of these brain activities and getting a view into the dynamics of brain activity. Two procedures are principally possible. First, one could use a combined EEG/neuroimaging (PET or fMRI) approach. PET or fMRI-activations could then be used to define the locations of dipole-sources and the corresponding activity curves of the dipoles could then be used in order to determine the sequence of activated brain areas. This procedure has already been introduced (Pouthas et al. 2000). Secondly, an independent localisation of ERP activity could be tried. This procedure would, however, only be reasonable if the results of the ERP localisation analysis were in good accordance with the results of the fMRI studies, using the same paradigm.

We describe here an investigation that is based on the latter strategy and uses an independent EEG source localisation. We have, therefore, analysed the averaged P300 data of fifty healthy volunteers with a tomographic localisation method, LORETA (Low Resolution Electromagnetic Tomography). This method was introduced in neurophysiological research in 1994 by Pascual-Marqui and consequently further developed in the following years (Pascual-Marqui et al. 1994; Pascual-Marqui 1999; Pascual-Marqui et al. 1999). This method has been used increasingly in the last years (Mulert et al. 2001, 2002, 2003) and earlier studies have demonstrated a high degree of consistence of LORETA studies and functional neuroimaging (Strik et al. 1998; Vitacco et al. 2002). An advantage of LORETA is that no assumptions have to be made about the number of active brain regions, which is necessary in a dipole source analysis (Scherg and Picton 1991).

Materials and methods

Subjects

Fifty healthy volunteers, 27 women and 23 men, without a history of neurological or psychiatric disorders and without recent drug consumption were studied (mean age = 36.5 ± 12.9 years; range 20–61 years). Exclusion criteria for the subjects were head injury in the history or any medication with influence on the central nervous system (e. g. cortisol, tranquillizers) in the last 3 months. After complete description of the study to the subjects, written informed consent was obtained. Auditory dysfunction was excluded by auditory testing of hearing threshold with a Philips audiometer.

Table 1 Common activation pattern of cortical regions in oddball paradigms using functional neuroimaging

	Left supramarginal gyrus	Right supramarginal gyrus	Anterior cingulate cortex	SMA and/or CMA	Right middle frontal gyrus	Right inferior frontal gyrus	Insula	Precuneus	Left superior temporal gyrus	Right superior temporal gyrus
Menon 1997	a	a	a	a						
Mc Carthy 1997	v	v	*	*	v	*	*	*	*	*
Linden 1999	v, a	v, a	v, a	v, a	a (sc)		v, a (bil)	a (bu)		
Stevens 2000	v, a	v, a	v, a	v,a	v, a	v, a	v, a (left)	v, a	a	a
Downar 2000	v, a, t	v, a, t	v, a, t	v, a, t		v, a, t	v, a, t (right)		a	a
Clark 2000	v	v	v	v	v	v	v (left)		v	
Kiehl 2001	a	a	a	a	a	a	a (bil)	a	a	a

v visual oddball; *a* auditory oddball; *t* tactile oddball; *bu* button press; *sc* silent counting; *bil* bilateral
* not or not sufficiently covered with the image slices of this study

Paradigm

An auditory oddball paradigm with 80 % non-target stimuli (400 tones, 500 Hz) and 20 % target stimuli (100 tones, 1000 Hz) presented binaurally through headphones in a pseudorandomised order was used (80 dB SPL, 40 ms duration with 10 ms rise and fall time, interstimulus interval 1.5 s). Subjects were seated with their eyes closed in a reclining chair and had to press a button with their dominant hand after target stimuli.

ERP-recording

Recording took place in a sound-attenuated and electrically shielded room adjacent to the recording apparatus (Neuroscan Synamps). Subjects were seated with closed eyes in a slightly reclined chair with a head rest. Evoked potentials were recorded with 33 electrodes referred to Cz (32 channels). The electrodes were positioned according to the International 10/20 system with the additional electrodes FC1, FC2, FC5, FC6, T1, T2, CP5, CP6, A1, A2, PO9, PO10. Fpz served as ground. Electrode impedance was less than 10 kohms. Data were collected with a sampling rate of 250 Hz and an analogous bandpass filter (0.16–50 Hz), and 200 ms pre-stimulus and 800 ms post-stimulus periods were evaluated. For artifact suppression, an amplitude criterium was used (±70 μV) involving all EEG channels and EOG at any time-point during the averaging period. Only waveshapes based on at least 50 averages were accepted.

Parametrization

We used two different approaches. First, we calculated LORETA-images for each ERP in the timeframe 230–480 ms post-stimulus. In the next step, these LORETA-images were averaged. This procedure has been used before (Anderer et al. 2003). However, it does not allow the time-courses to be displayed, as was intended in the presented study (Fig. 6). Therefore, we additionally calculated a LORETA-image, based on the grand average of the ERPs, using the LORETA–"Explorer" and allowing a time-course display.

LORETA

LORETA assumes that the smoothest of all activity distributions is the most plausible ("smoothness assumption") and, therefore, a particular current density distribution is found. This fundamental assumption of LORETA directly relies on the neurophysiological observation of coherent firing of neighbouring cortical neurons during stimulus processing (Llinas 1988; Gray et al. 1989; Silva et al. 1991) and can, therefore, be seen as a physiologically based constraint. However, this coherent firing has been described on the level of cortical columns, which have a much smaller diameter than the voxels used in the LORETA software; the empirical basis for coherent firing in the millimetre range is not strong enough to fully accept this constraint as a physiological one, even if it might help to produce useful results. The characteristic feature of the resulting solution is its relatively low spatial resolution, which is a direct consequence of the smoothness constraint. Specifically, the solution produces a "blurred-localised" image of a point source, conserving the location of maximal activity, but with a certain degree of dispersion. It should be emphasised that this solution will typically produce a "blurred-localised" image of arbitrary distributions due to the principle of superposition. However, some distributions of point sources may superpose in such a way that they actually cancel out on the scalp and cannot, therefore, be correctly localised by any method. The version of LORETA used in the present study used the digitised Talairach atlas (Talairach and Tournoux 1988) available as digitised MRI from the Brain Imaging Centre, Montreal Neurologic Institute, estimating the current source density (microAmperes/mm^2) distribution for either single timepoints or epochs of brain electric activity on a dense grid of 2394 voxels at 7 mm spatial resolution (Pascual-Marqui et al. 1999). The solution space (the three-dimensional space where the inverse EEG problem is solved) was restricted to the grey matter and hippocampus in the Talairach atlas (anatomically based constraint). Localisation with regard to spherical and realistic head geometry was done using EEG electrode coordinates reported by Towle et al. (1993). A voxel was labelled as grey matter if it met the following three conditions: its probability of being grey matter was higher than that of being white matter, its probability of being grey matter was higher than that of being cerebrospinal fluid, and its probability of being grey matter was higher than 33 % (Pascual-Marqui et al. 1999).

Results

Grand averages of auditory P300 referenced to common average are shown in Figs. 1 and 2. The amplitude of the P300 peak was 5.2 μV and the latency 348 ms, measured at Pz, respectively 2.2 μV and 316 ms, measured at Fz. Corresponding to the time-course of the Global Field Power (GFP, see Fig. 3), we selected the timeframe 230–480 ms post-stimulus for further analyses.

Concerning the average of the LORETA-files, based on the individual ERPs, the maximal current source density value was found in the supplementary motor area (SMA), Talairach coordinates (x, y, z): –3, –11, 64. Further activations were in the bilateral inferior parietal lobe (–45, –39, 50 and 46, –32, 50), the anterior cingulate cortex (ACC, –3, 45, –6), the bilateral superior temporal gyrus (STG), larger on the left (–59, –25, 15) than on the right (60, –32, 15), the right insula (46, 10, 1) and the bilateral middle frontal cortex (46, 10, 36 and –45, 3, 43) and in the precuneus (4, –67, 29).

Very similar activation patterns were found in the LORETA analysis of the ERP-grand average with the maximal activations in the SMA, the bilateral inferior parietal lobe/the temporo-parietal junction, larger on the left, the ACC, the bilateral superior temporal gyrus (STG), larger on the left, the right insula and the bilateral middle and right inferior frontal cortex and the precuneus (Table 2, Figs. 4 and 5). Because of the similarity between both averaging approaches, we only used the LORETA analysis of the ERP-grand average for further analyses. In the next step, we analysed the time-courses of these regions (Fig. 6). Here, the current source density values are shown for the voxels with the same coordinates as in Table 2, i. e. the voxels with maximal current source density values in the respective region in the LORETA analysis.

Finally, we divided the P300 time-frame into five 50 ms steps and analysed the average data with LORETA (Table 3). These results are in fine accordance with the time-course analysis as shown in Fig. 6. For example, the SMA shows an early activation maximum after 230–280 ms, is then not active after 330–380 ms, and shows a second maximum after 380–430 ms and 430–480 ms post-stimulus. The precuneus shows an activation between 330 and 380 ms, which can be seen both in the 50 ms window analysis (Table 3) and in the time-course analysis (Table 3). With regard to the early P300 component (P3a) and the main P3 component (P3b), it can be seen (Fig. 6) that most of the related brain regions contribute

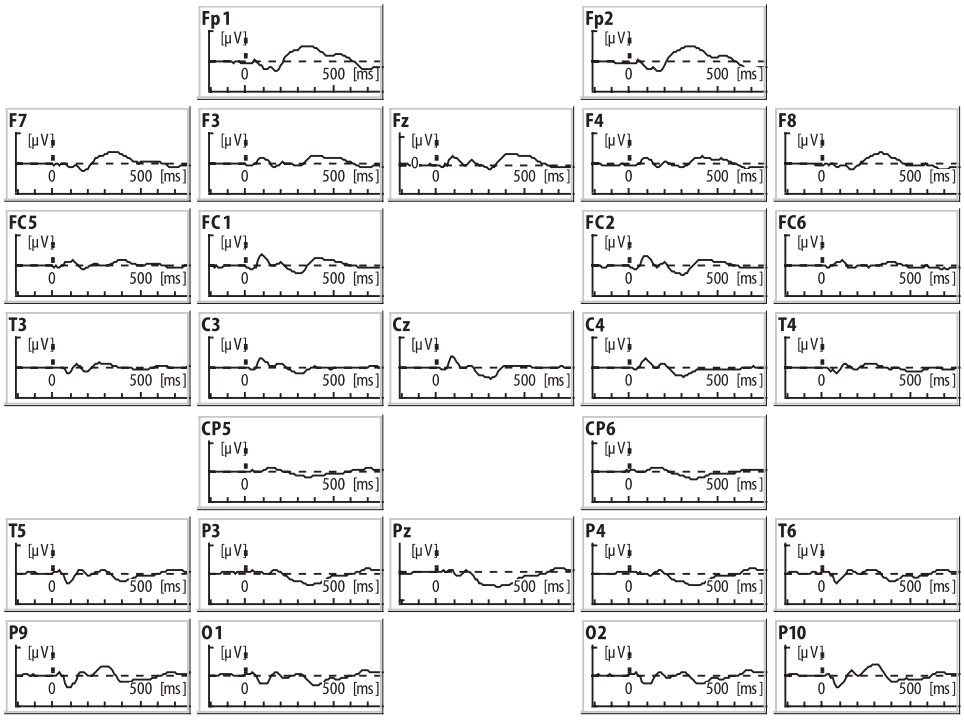

Fig. 1 Grand average of the auditory evoked potentials of all healthy subjects (n = 50)

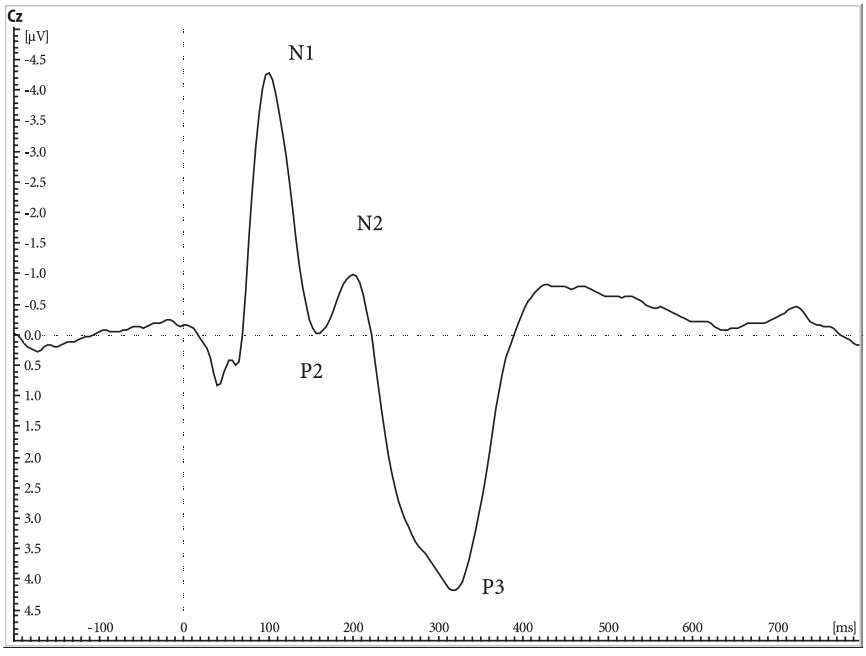

Fig. 2 Grand average measured at Cz. A positive component with a peak around 300 ms post-stimulus can easily be detected

to the early part of the P300, but only the SMA/CMA, the inferior parietal lobe and, to some degree, the left middle frontal gyrus contribute substantially to the late part of the P300. It can also be seen that even if the GFP suggests a timeframe between 230 and 480 ms for the P300, no single involved brain region exactly follows these time values, but shows distinct time-courses.

Discussion

The locations of the current density maxima in the present study are in good accordance with previous results of intracranial electrophysiological studies (Halgren et al. 1998) and functional neuroimaging studies (Table 1). This is noteworthy, since to our knowledge no earlier studies dealing with EEG scalp data have found such a high degree of accordance with functional imaging data

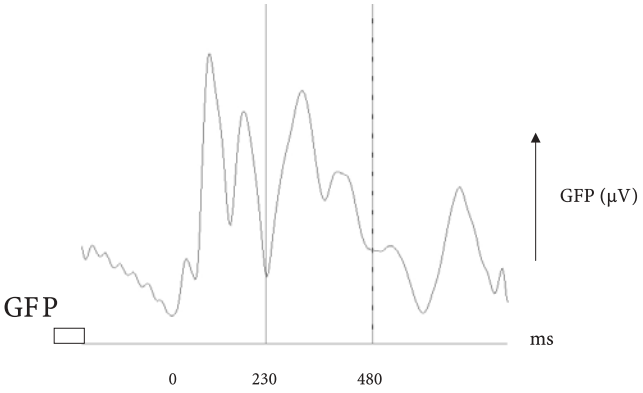

Fig. 3 Global Field Power (GFP) of the grand average data

(Yamazaki et al. 2000; Jentzsch and Sommer 2001; Yamazaki et al. 2001) and intracranial recordings (Halgren et al. 1998). Main findings in the fMRI studies have been activations in the temporo-parietal junction (TPJ), the supplementary motor cortex (SMA) and the anterior cingulate cortex (ACC), the superior temporal gyrus (STG), the insula and the right middle frontal gyrus. The same regions were found in the present study. Some authors have also described an activation of the precuneus (Linden et al. 1999; Stevens et al. 2000; Kiehl et al. 2001), as was found with LORETA. Regarding the activation of the temporo-parietal junction, in some studies a left > right asymmetry has been described, as found in the present study (Menon et al. 1997; Kiehl et al. 2001), while others have seen an asymmetry in the opposite direction (Downar et al. 2000) or no clear difference between the hemispheres (Linden et al. 1999). An activation of the superior temporal gyrus, as seen in the present study with an auditory oddball paradigm, has been described in fMRI studies using auditory oddball paradigms (Downar et al. 2000; Stevens et al. 2000), but also once in a visual oddball experiment (Clark et al. 2000). In the present study, we saw a strong activation of the right insula, as described earlier (Downar et al. 2000). However, other authors have described a pronounced activation of the left insula (Clark et al. 2000; Stevens et al. 2000) or bilateral activation (Kiehl et al. 2001).

So far, the precise relationship between functional imaging studies, based on brain blood supply and EEG data has not been resolved. However, recent studies have revealed a close relationship between the BOLD (blood

Table 2 Brain regions showing activation in response to task relevant stimuli in the oddball task (230–480 ms post-stimulus)

Brain region	Brodmann area	Talairach			Current source density ($\mu A/mm^2 \times 10^{-3}$)
		x	y	z	
SMA/CMA	6	4	–4	50	1.85
L inferior parietal lobe	40	–45	–39	50	1.45
L superior temporal gyrus	42	–59	–32	8	1.35
R superior temporal gyrus/TPJ	22	60	–39	15	1.25
L middle temporal gyrus	21	–59	–18	–13	1.23
ACC	32	–3	45	–6	1.09
R insula	13	46	10	1	1.08
L middle frontal gyrus	6	–24	3	57	0.99
R middle frontal gyrus	9	46	10	36	0.94
Precuneus	31	4	–67	29	0.94
R inferior frontal gyrus	44	53	17	22	0.94

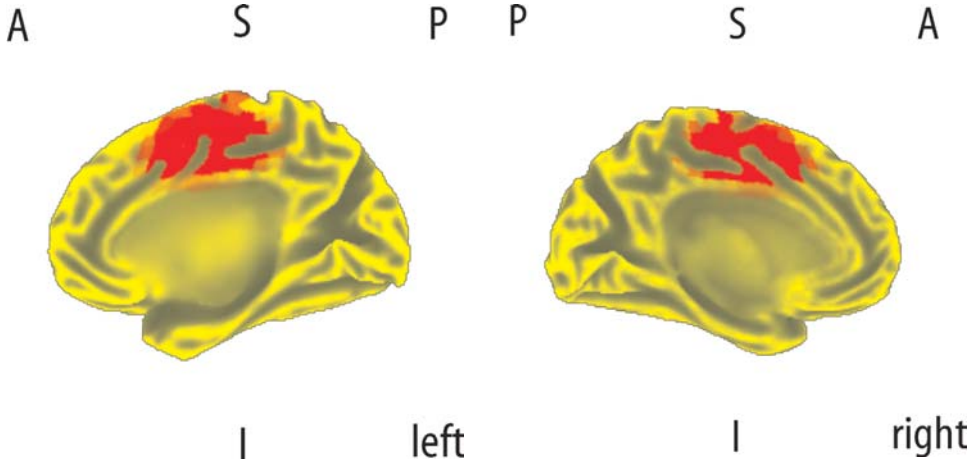

Fig. 4 Grand average (n = 50) three dimensional maps of current density for targets in the time-frame between 230 and 480 ms superimposed on an inflated cortex. Lateral views (*A* anterior; *P* posterior; *S* superior; *I* inferior)

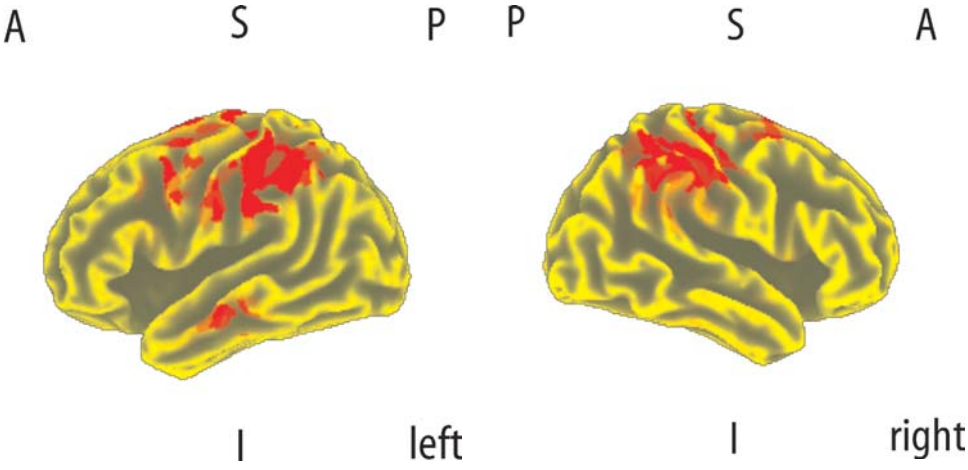

Fig. 5 Grand average (n = 50) three dimensional maps of current density for targets in the time-frame between 230 and 480 ms superimposed on an inflated cortex. Medial views (*A* anterior; *P* posterior; *S* superior; *I* inferior)

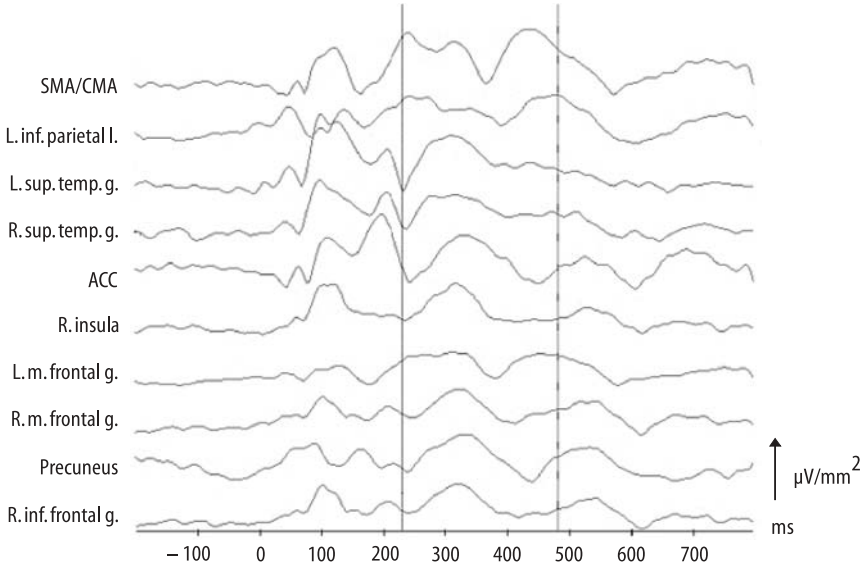

Fig. 6 Current source density time-course of the main active regions underlying the P300 potential, based on the grand average data of all healthy subjects (n = 50). The vertical lines indicate the time-frame between 230 and 480 ms. Different brain areas show different time-courses, contributing to early parts of the P300, to late parts or both

oxygenation level dependent)-effect, which is the physiological basis of fMRI, and neuronal field potentials (local field potentials = LFP) (Logothetis et al. 2001). Clearly, the occurrence of local field potentials does not imply that the same signal is measurable on the scalp surface. This does also depend on the source configuration and on synchronisation. In order to get a measurable signal on the scalp, the neural population should activate coherently in space and time. However, if a clear potential can be detected on the scalp over a certain time, as in the case of the P300, a clear BOLD response should be associated and detectable. With these limitations, therefore, it could be postulated that differences between fMRI activation clusters and EEG inverse solutions are in many cases due to deficiencies of these EEG-based localisations and not due to relevant differences in the topography of the underlying physiological processes, i. e. between electrical activity of neurons and blood supply of brain tissue. Differences between the localisations of the generators of the P300, described on the basis of EEG scalp data and on fMRI, may, thus, be a consequence of deficiencies of the applied EEG-localisation technique. However, some distributions of point sources may superpose in such a way that they actually cancel out on the scalp and, therefore, cannot be correctly localised by any method. With dipole source analysis, the number of active brain regions must be defined. This is a critical point, since no correct solution can be found if the number of dipoles is not correct. An advantage of LORETA is that no such assumption has to be made. However, if the assumptions about the number and location of active electrical sources are correct (e. g. taken from parallel fMRI or PET imaging), a dipole model can well be used to explain the time-course of the EEG scalp data (Pouthas et al. 2000). In summary, the good accordance of the locations of activity in the present study with the fMRI literature is the crucial point in order to use this analysis as starting point for a next step, i. e. the analysis of the time architecture of the brain activation. Here, the EEG is the method of choice, since it allows a time resolution in the range of milliseconds. In a previous study by Pouthas et al., with a dipole model

Table 3 Maximum activations in response to task relevant stimuli in the oddball task (230–480 ms post-stimulus): focus on the time-course

Brain region	Brodmann area	Talairach			Current source density ($\mu A/mm^2 \times 10^{-3}$)
		x	y	z	
230–280 ms					
SMA/CMA	6	–3	–4	57	2.06
L inferior parietal lobe	40	–45	–39	50	1.77
L middle temporal gyrus	21	–59	–18	–13	1.47
R superior temporal gyrus/TPJ	22	60	–39	15	1.14
L middle frontal gyrus	6	–24	–4	57	1.13
280–330 ms					
L superior temporal gyrus	42	–59	–32	8	2.02
ACC	24	4	3	43	1.89
R insula	13	46	10	1	1.77
R superior temporal gyrus/TPJ	39	53	–53	15	1.77
Medial frontal gyrus	11	–3	38	–13	1.69
330–380 ms					
ACC	32	–3	45	–6	1.72
L superior temporal gyrus	42	–59	–32	15	1.50
Precuneus	31	4	–67	22	1.41
R superior temporal gyrus/TPJ	22	60	–39	15	1.40
L middle temporal gyrus	21	–52	3	–20	1.33
380–430 ms					
SMA/CMA	6	–3	–11	57	2.0
L middle temporal gyrus	21	–59	–18	–13	1.11
L superior temporal gyrus	42	–59	–25	8	1.09
L inferior parietal lobe	40	–45	–39	50	1.09
R superior temporal gyrus	42	60	–25	15	1.07
430–480 ms					
SMA/CMA	6	4	–4	50	2.24
L inferior parietal lobe	40	–45	–39	50	1.79
L middle frontal gyrus	6	–24	–4	57	1.16
R superior temporal gyrus/TPJ	22	60	–39	22	1.06
R inferior parietal lobe	40	46	–32	50	1.06

with the dipoles seated in the activations found with PET ("PET dipolar model"), interesting reports could be made about different time-courses of the prefrontal cortex and cingulate activations under different conditions in a visual discrimination task (Pouthas et al. 2000). Our present study uses a different approach, namely, an independent EEG-source analysis, where current source density locations are not primarily defined by functional imaging, but are nevertheless in good accordance with the common fMRI activation patterns reported in the literature.

As can be seen in Fig. 6, there are some regions with an activation time-course that is closely related to the scalp-P300 potential (e. g. the ACC and the precuneus), some with an earlier decrease of activation (e. g. the right insula and the right middle frontal gyrus) and some with two or more peaks within the timeframe of the P300 potential (e. g. the SMA/CMA and the left inferior parietal lobe). Interestingly, the activations in the earlier time-frames are also in good accordance with the literature; there is a strong activation of the superior temporal gyrus during the time-frame of the N1 with some overlap here with SMA and ACC activation and a strong contribution of the ACC to the N2.

Comparing these results to the findings of Halgren et al. (Halgren et al. 1995a, 1995b, 1998), it should be emphasised that these results are often discussed in an oversimplified way, attributing the activation of the cingulate cortex, the dorsolateral prefrontal cortex and the supramarginal gyrus to the P3a, and the activations around the superior temporal sulcus, of the posterior superior parietal cortex and the medial temporal cortex to the P3b. In fact, the findings have been more complex, describing three peaks as a widespread triphasic waveform in the frontal lobe at 210–220, 280–320 and 390–420 ms post-stimulus, assigned to the scalp N2a, P3a and slow wave, respectively (Baudena et al. 1995). Interestingly, a similar time-course can be seen in the SMA/CMA and the anterior cingulate cortex in our data, with the N2a peaking earlier in the ACC. The activations in the dorsolateral prefrontal cortex in our data set show three activation peaks only on the right side (right middle and inferior frontal gyrus) with the second and third peak later than in the intracranial recordings. On the left side, in the left middle frontal cortex, the first activation covers the time range of N2a and P3a, but the second peaks in the time range of the slow wave. Concerning the P3b, intracranial recordings show strong activation in the anterior hippocampus and posterior parietal cortex. The contribution of the anterior hippocampus to the scalp EEG is probably small and

has not been detected in this investigation. Also, the posterior parietal activation is circumscribed. Here, the limited spatial resolution of LORETA/smoothness assumption might be the reason why this activation partly contributes to the late activation part of the inferior parietal cortex in the present investigation. Interestingly, activations of the hippocampus which are prominent in intracranial recordings, but not in the present study based on scalp EEG data are also typically not detected in the fMRI investigations. However, Kiehl et al. have described P300-related activations in the hippocampus (2001). The rare findings of the hippocampus region in P300-fMRI studies may accordingly be (apart from an insufficient coverage with the field of view) a consequence of susceptibility artefacts near the skull base and, therefore, not related to the results of the present study. In the present study, no activations of the thalamus could be described since this region is not included in the solution space (the three-dimensional space where the inverse EEG problem is solved), which was restricted to the grey matter and hippocampus in the Talairach atlas. Activations of the thalamus, however, have been a common finding in P300-fMRI experiments (Clark et al. 2000; Kiehl et al. 2001)

Time-course analysis based on EEG data has a clear advantage in comparison to event-related fMRI time-course analysis, because of its superior time resolution, which can also be used in some cases for "mental chronometry" (Formisano et al. 2002). However, one advantage of an fMRI time-course analysis would be that it also allows to some degree a time-course analysis of subcortical structures, which cannot be analysed with ERP-based methods (e. g. the thalamus or striatum). Additionally, it would allow a differential time-course analysis of brain structures, which are spatially closely neighboured, but functionally different. Here, the limited spatial resolution of the LORETA analysis would not allow convincing results.

Time-course information might be helpful in order to better understand attenuations of the P300 potential in diseases like Alzheimer dementia or schizophrenia. So far, studies have revealed differences in the amplitude or latency of the scalp P3a, or P3b, but a clear correlation of these reports to the underlying brain regions has not been possible (Iwanami et al. 2002). With the LORETA time-course analysis, it might be possible to detect not only the failure of brain regions to activate, but also a disturbed time architecture, with tardy activations or disturbed synchronisation of brain regions. Especially neurocognitive deficits, which are a common finding in schizophrenia (Moritz et al. 2002), may be related to a disturbed synchronisation (Green and Nuechterlein 1999).

Conclusion

Tomographic analysis of the neural generators of the P300 potential with LORETA is in good accordance with both intracranial recordings and recent fMRI studies. In addition to the detection of the brain structures, generating the P300 potential, the high temporal resolution of the EEG allows a precise description of the activation time-course in these regions of interest. Distinct time-course patterns of activation are clearly detectable. This might be helpful for a better understanding of attenuations in the P300 amplitude or latency in brain/mental diseases like Alzheimer dementia or schizophrenia.

References

1. Anderer P, Saletu B, Semlitsch HV, Pascual-Marqui RD (2003) Non-invasive localization of P300 sources in normal aging and age-associated memory impairment. Neurobiol Aging 24: 463–479
2. Baudena P, Halgren E, Heit G, Clarke JM (1995) Intracerebral potentials to rare target and distractor auditory and visual stimuli. III. Frontal cortex. Electroencephalogr Clin Neurophysiol 94: 251–264
3. Blackwood D (2000) P300, a state and a trait marker in schizophrenia (In Process Citation). Lancet 355:771–772
4. Burock MA, Buckner RL, Woldorff MG, Rosen BR, Dale AM (1998) Randomized event-related experimental designs allow for extremely rapid presentation rates using functional MRI. Neuroreport 9:3735–3739
5. Clark VP, Fannon S, Lai S, Benson R, Bauer L (2000) Responses to rare visual target and distractor stimuli using event-related fMRI. J Neurophysiol 83:3133–3139
6. Dierks T, Maurer K (1989) P300 evoked by an auditory and a visual paradigm and a semantic task. Psychiatry Res 29:439–441
7. Downar J, Crawley AP, Mikulis DJ, Davis KD (2000) A multimodal cortical network for the detection of changes in the sensory environment (In Process Citation). Nat Neurosci 3:277–283
8. Formisano E, Linden DE, Di Salle F, Trojano L, Esposito F, Sack AT, Grossi D, Zanella FE, Goebel R (2002) Tracking the mind's image in the brain. I. Time-resolved fMRI during visuospatial mental imagery. Neuron 35:185–194
9. Friston KJ, Fletcher P, Josephs O, Holmes A, Rugg MD, Turner R (1998) Event-related fMRI: characterizing differential responses. Neuroimage 7:30–40
10. Frodl-Bauch T, Bottlender R, Hegerl U (1999) Neurochemical substrates and neuroanatomical generators of the event-related P300. Neuropsychobiology 40:86–94
11. Gallinat J, Riedel M, Juckel G, Sokullu S, Frodl T, Moukhtieva R, Mavrogiorgou P, Nissle S, Muller N, Danker-Hopfe H, Hegerl U (2001) P300 and symptom improvement in schizophrenia. Psychopharmacology (Berl) 158:55–65
12. Gray CM, Konig P, Engel AK, Singer W (1989) Oscillatory responses in cat visual cortex exhibit inter-columnar synchronization which reflects global stimulus properties. Nature 338: 334–337
13. Green MF, Nuechterlein KH (1999) Cortical oscillations and schizophrenia: timing is of the essence. Arch Gen Psychiatry 56:1007–1008
14. Halgren E, Baudena P, Clarke JM, Heit G, Liegeois C, Chauvel P, Musolino A (1995a) Intracerebral potentials to rare target and distractor auditory and visual stimuli. I. Superior temporal plane and parietal lobe. Electroencephalogr Clin Neurophysiol 94: 191–220
15. Halgren E, Baudena P, Clarke JM, Heit G, Marinkovic K, Devaux B, Vignal JP, Biraben A (1995b) Intracerebral potentials to rare target and distractor auditory and visual stimuli. II. Medial, lateral and posterior temporal lobe. Electroencephalogr Clin Neurophysiol 94:229–250
16. Halgren E, Marinkovic K, Chauvel P (1998) Generators of the late cognitive potentials in auditory and visual oddball tasks. Electroencephalogr Clin Neurophysiol 106:156–164
17. Hegerl U, Frodl-Bauch T (1997) Dipole source analysis of P300 component of the auditory evoked potential: a methodological advance? Psychiatry Res 74:109–118

18. Hegerl U, Juckel G, Muller-Schubert A, Pietzcker A, Gaebel W (1995) Schizophrenics with small P300: a subgroup with a neurodevelopmental disturbance and a high risk for tardive dyskinesia? Acta Psychiatr Scand 91:120–125
19. Higashima M, Urata K, Kawasaki Y, Maeda Y, Sakai N, Mizukoshi C, Nagasawa T, Kamiya T, Yamaguchi N, Koshino Y (1998) P300 and the thought disorder factor extracted by factor-analytic procedures in schizophrenia. Biol Psychiatry 44:115–120
20. Horn H, Syed N, Lanfermann H, Maurer K, Dierks T (2003) Cerebral networks linked to the event-related potential P300. Eur Arch Psychiatry Clin Neurosci 253:154–159
21. Iwanami A, Kato N, Kasai K, Kamio S, Furukawa S, Fukuda M, Nakagome K, Araki T, Okajima Y, Isono H, Kamijima K (2002) P300 amplitude over temporal regions in schizophrenia. Eur Arch Psychiatry Clin Neurosci 252:1–7
22. Jentzsch I, Sommer W (2001) Sequence-sensitive subcomponents of P300: topographical analyses and dipole source localization. Psychophysiology 38:607–621
23. Juckel G, Muller-Schubert A, Gaebel W, Hegerl U (1996) Residual symptoms and P300 in schizophrenic outpatients. Psychiatry Res 65:23–32
24. Kiehl KA, Laurens KR, Duty TL, Forster BB, Liddle PF (2001) Neural sources involved in auditory target detection and novelty processing: an event-related fMRI study. Psychophysiology 38: 133–142
25. Linden DE, Prvulovic D, Formisano E, Vollinger M, Zanella FE, Goebel R, Dierks T (1999) The functional neuroanatomy of target detection: an fMRI study of visual and auditory oddball tasks. Cereb Cortex 9:815–823
26. Llinas RR (1988) The intrinsic electrophysiological properties of mammalian neurons: insights into central nervous system function. Science 242:1654–1664
27. Logothetis NK, Pauls J, Augath M, Trinath T, Oeltermann A (2001) Neurophysiological investigation of the basis of the fMRI signal. Nature 412:150–157
28. McCarthy G, Luby M, Gore J, Goldman-Rakic P (1997) Infrequent events transiently activate human prefrontal and parietal cortex as measured by functional MRI. J Neurophysiol 77:1630–1634
29. Menon V, Ford JM, Lim KO, Glover GH, Pfefferbaum A (1997) Combined event-related fMRI and EEG evidence for temporal-parietal cortex activation during target detection. Neuroreport 8:3029–3037
30. Moritz S, Andresen B, Perro C, Schickel M, Krausz M, Naber D (2002) Neurocognitive performance in first-episode and chronic schizophrenic patients. Eur Arch Psychiatry Clin Neurosci 252: 33–37
31. Mulert C, Gallinat J, Dorn H, Herrmann WM, Winterer G (2003) The relationship between reaction time, error rate and anterior cingulate cortex activity. Int J Psychophysiol 47:175–183
32. Mulert C, Gallinat J, Pascual-Marqui R, Dorn H, Frick K, Schlattmann P, Mientus S, Herrmann WM, Winterer G (2001) Reduced event-related current density in the anterior cingulate cortex in schizophrenia. Neuroimage 13:589–600
33. Mulert C, Juckel G, Augustin H, Hegerl U (2002) Comparison between the analysis of the loudness dependency of the auditory N1/P2 component with LORETA and dipole source analysis in the prediction of treatment response to the selective serotonin reuptake inhibitor citalopram in major depression. Clin Neurophysiol 113:1566–1572
34. Pascual-Marqui RD (1999) Review of methods for solving the EEG inverse problem. Int J Bioelectromagnetism 1:75–86
35. Pascual-Marqui RD, Lehmann D, Koenig T, Kochi K, Merlo MC, Hell D, Koukkou M (1999) Low resolution brain electromagnetic tomography (LORETA) functional imaging in acute, neuroleptic-naive, first-episode, productive schizophrenia. Psychiatry Res 90:169–179
36. Pascual-Marqui RD, Michel CM, Lehmann D (1994) Low resolution electromagnetic tomography: a new method for localizing electrical activity in the brain. Int J Psychophysiol 18:49–65
37. Pouthas V, Garnero L, Ferrandez AM, Renault B (2000) ERPs and PET analysis of time perception: spatial and temporal brain mapping during visual discrimination tasks. Hum Brain Mapp 10:49–60
38. Roth WT, Cannon EH (1972) Some features of the auditory evoked response in schizophrenics. Arch Gen Psychiatry 27: 466–471
39. Scherg M, Picton TW (1991) Separation and identification of event-related potential components by brain electric source analysis. Electroencephalogr Clin Neurophysiol Suppl 42:24–37
40. Silva LR, Amitai Y, Connors BW (1991) Intrinsic oscillations of neocortex generated by layer 5 pyramidal neurons. Science 251: 432–435
41. Stevens AA, Skudlarski P, Gatenby JC, Gore JC (2000) Event-related fMRI of auditory and visual oddball tasks. Magn Reson Imaging 18:495–502
42. Strik WK, Fallgatter AJ, Brandeis D, Pascual-Marqui RD (1998) Three-dimensional tomography of event-related potentials during response inhibition: evidence for phasic frontal lobe activation. Electroencephalogr Clin Neurophysiol 108:406–413
43. Talairach J, Tournoux P (1988) Co-planar stereotaxic atlas of the human brain. Thieme, Stuttgart
44. Towle VL, Bolanos J, Suarez D, Tan K, Grzeszczuk R, Levin DN, Cakmur R, Frank SA, Spire JP (1993) The spatial location of EEG electrodes: locating the best-fitting sphere relative to cortical anatomy. Electroencephalogr Clin Neurophysiol 86:1–6
45. Vitacco D, Brandeis D, Pascual-Marqui R, Martin E (2002) Correspondence of event-related potential tomography and functional magnetic resonance imaging during language processing. Hum Brain Mapp 17:4–12
46. Winterer G, Mulert C, Mientus S, Gallinat J, Schlattmann P, Dorn H, Herrmann WM (2001) P300 and LORETA: comparison of normal subjects and schizophrenic patients. Brain Topogr 13: 299–313
47. Yamazaki T, Kamijo K, Kenmochi A, Fukuzumi S, Kiyuna T, Takaki Y, Kuroiwa Y (2000) Multiple equivalent current dipole source localization of visual event-related potentials during oddball paradigm with motor response. Brain Topogr 12:159–175
48. Yamazaki T, Kamijo K, Kiyuna T, Takaki Y, Kuroiwa Y (2001) Multiple dipole analysis of visual event-related potentials during oddball paradigm with silent counting. Brain Topogr 13:161–168